catalysts

MDPI

Article

Microwave-Assisted Synthesis of 1,4-Dihydropyridines via the Hantzsch Reaction Using a Recyclable HPW/PEG-400 Catalytic System

Wender Alves Silva [1,*], Sayuri Cristina Santos Takada [2], Claudia Cristina Gatto [3] and Izabella Vitoria Maravalho [1]

[1] Laboratory for Bioactive Compound Synthesis, Campus Universitario Darcy Ribeiro, University of Brasilia (IQ-UnB), Brasilia 70904-970, Brazil; izabellavitoria22@hotmail.com
[2] Embrapa Genetic Resources and Biotechnology, Empresa Brasileira de Pesquisa Agropecuaria, Brasilia 70770-917, Brazil; sayuri.takada@embrapa.br
[3] Laboratory of Inorganic Synthesis and Crystallography, University of Brasilia (IQ-UnB), Brasilia 70904-970, Brazil; ccgtto@gmail.com
* Correspondence: wender.silva@unb.br

Abstract

1,4-Dihydropyridines (1,4-DHPs) are privileged heterocycles with broad relevance in medicinal chemistry and redox-related applications. However, conventional Hantzsch syntheses typically require prolonged thermal heating and often suffer from limited efficiency and regioselectivity. Herein, we report a sustainable and efficient microwave-assisted protocol for the synthesis of 1,4-DHPs, employing phosphotungstic acid (HPW) as a heteropolyacid catalyst in PEG-400 as a green reaction medium. The multicomponent cyclocondensation proceeds rapidly under microwave irradiation, affording the desired 1,4-DHP derivatives in good to excellent yields within short reaction times. Compared with classical acid-catalyzed conditions, the HPW/PEG-400 system markedly enhances regioselectivity toward the 1,4-DHP framework while simultaneously reducing energy input. Moreover, the catalytic system exhibits good recyclability, underscoring its potential as a practical and environmentally responsible platform for the synthesis of bioactive 1,4-dihydropyridine scaffolds.

Keywords: 1,4-dihydropyridines; multicomponent reaction; phosphotungstic acid; heteropolyacid catalyst; PEG-400; microwave-assisted organic synthesis

Academic Editors: Kotohiro Nomura, Raffaella Mancuso, Mário Manuel Quialheiro Simões and Werner Oberhauser

Received: 30 December 2025
Revised: 15 January 2026
Accepted: 16 January 2026
Published: 17 January 2026

1. Introduction

Since their discovery, pyridine and its reduced analogs have played a central role in the development of heterocyclic chemistry [1,2]. Among these, 1,2-dihydropyridines (1,2-DHPs) and 1,4-dihydropyridines (1,4-DHPs) have emerged as particularly valuable scaffolds due to their broad spectrum of biological and pharmacological activities (Figure 1) [3–6].

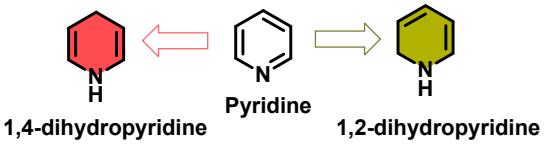

Figure 1. Schematic representation of the two possible regioisomers of dihydropyridines (1,4-DHP and 1,2-DHP).

Several alkaloids, such as dioscorine, employ 1,2-dihydropyridines (1,2-DHPs) as pivotal precursors for constructing the isoquinuclidine framework [7,8]. In addition, an isoquinuclidine intermediate generated from a 1,2-DHP serves as an essential step in the synthesis of oseltamivir phosphate (Tamiflu®), a well-known antiviral agent (Scheme 1). Consequently, 1,2-DHP scaffolds represent valuable intermediates and building blocks in modern pharmaceutical chemistry [9].

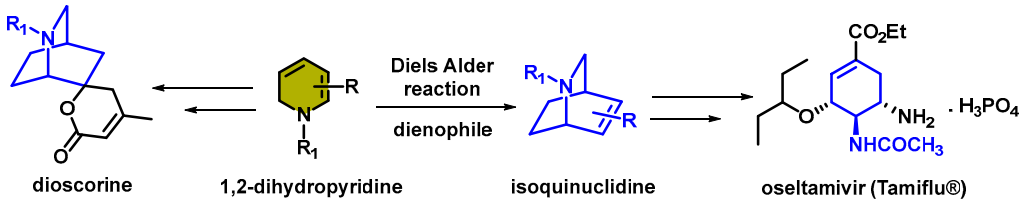

Scheme 1. Structure of 1,2-dihydropyridine (1,2-DHP) and the key isoquinuclidine intermediate involved in the synthesis of pharmacologically relevant compounds.

The 1,4-dihydropyridine (1,4-DHP) scaffold is widely recognized as a privileged structure in medicinal chemistry, serving as a versatile template for the design of bioactive molecules with significant therapeutic potential [10–13]. Naturally occurring derivatives, such as nicotinamide adenine dinucleotide (NADH) and its phosphorylated analog nicotinamide adenine dinucleotide phosphate (NADPH), exemplify the biological importance of this structural motif and its central role in redox biochemistry (Figure 2) [14,15]. According to the International Union of Pure and Applied Chemistry (IUPAC), privileged scaffolds exhibit structural diversity, featuring a semi-rigid core capable of accommodating multiple hydrophobic substituents without hydrophobic collapse—an architectural characteristic that often confers favorable drug-like properties [16].

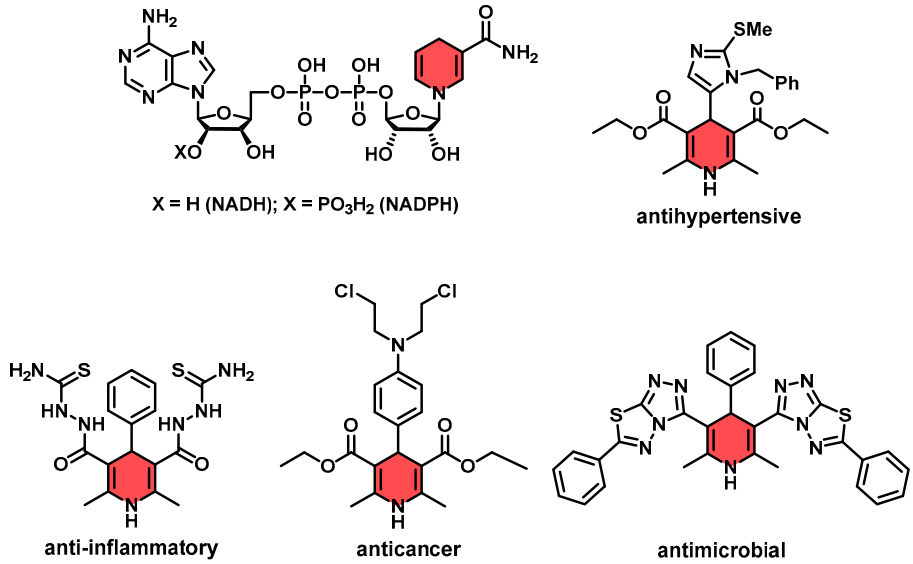

Figure 2. Structures of 1,4-dihydropyridine (1,4-DHP), NADH/NADPH, and selected medicinally important compounds derived from DHP scaffolds.

A bibliometric survey of 1,4-DHP derivatives retrieved from PubMed (Figure 3) highlights the historical evolution of the field: interest rose from the late 1960s through the 1970s–1990s and has since moderated, averaging ~50 publications per year over the last decade. This trajectory underscores the value of consolidating and revitalizing the area through comprehensive, up-to-date analyses. Despite long-standing pharmacological importance, systematic reviews remain scarce [17], with only a few focused on specific therapeutic domains [10–16].

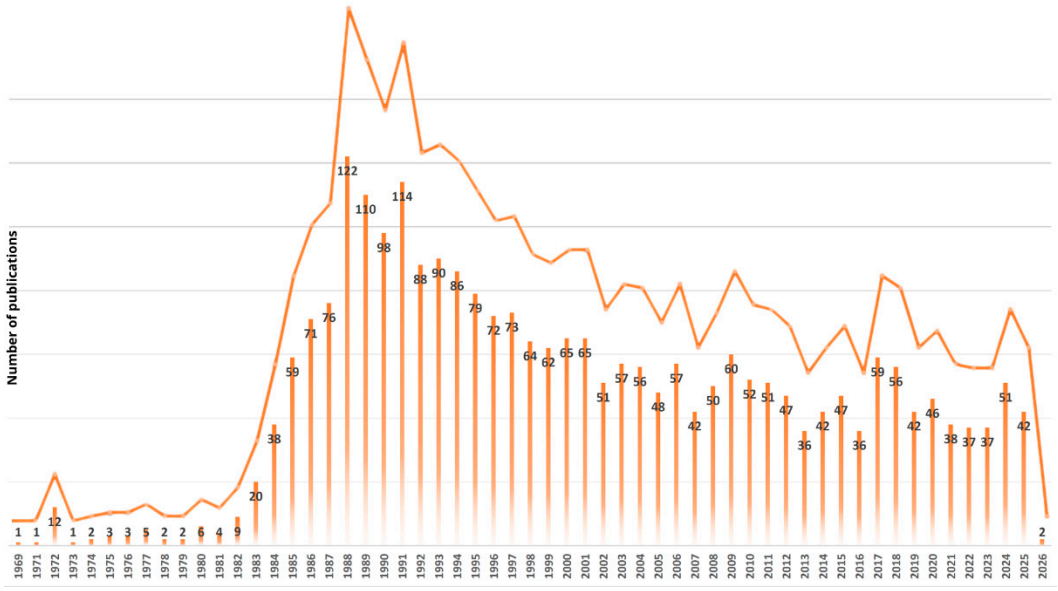

Figure 3. The number of publications published on 1,4-DHP scaffolds since 1969. https://pubmed.ncbi.nlm.nih.gov/?term=1,4-dihydropyridine (accessed 14 January 2026).

Pharmacologically, 1,4-DHPs are best known as calcium-channel blockers (CCBs) used in the management of hypertension and other cardiovascular disorders, owing to their ability to modulate vascular smooth-muscle contraction and reduce blood pressure (Figure 4) [13,18–22].

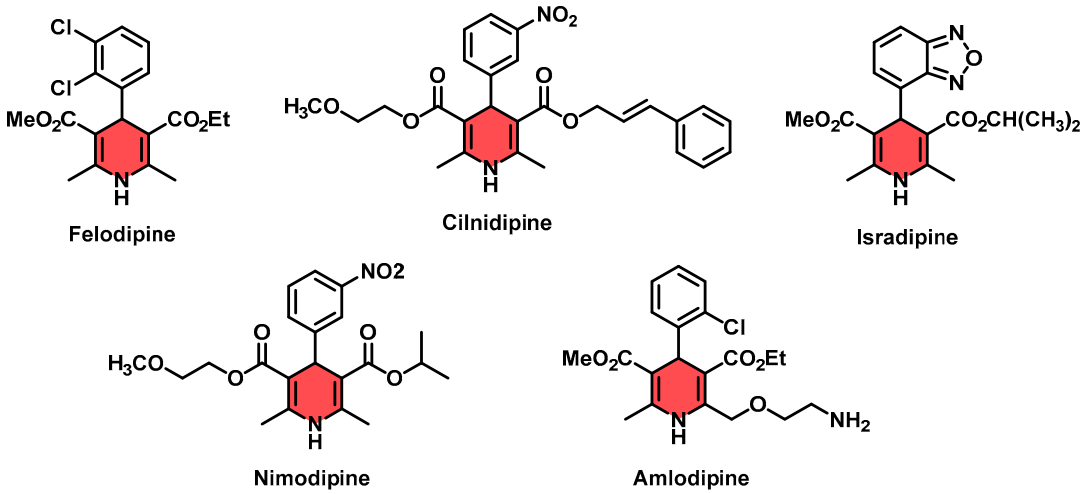

Figure 4. Examples of pharmaceuticals containing the 1,4-dihydropyridine (1,4-DHP) scaffold.

Hantzsch's pioneering work on the synthesis of 1,4-DHPs involved the condensation of aldehydes with two equivalents of ethyl acetoacetate and ammonia in a one-pot multicomponent reaction (MCR), establishing the foundation for modern 1,4-DHP chemistry. Classically, 1,4-DHPs are obtained through the Hantzsch MCR, first reported by Arthur Rudolf Hantzsch in 1882. This cyclocondensation between a β-ketoester, an aldehyde, and ammonia yields symmetric 1,4-DHPs—commonly referred to as *Hantzsch esters* (Scheme 2)—which remain cornerstone intermediates in synthetic and medicinal organic chemistry [23].

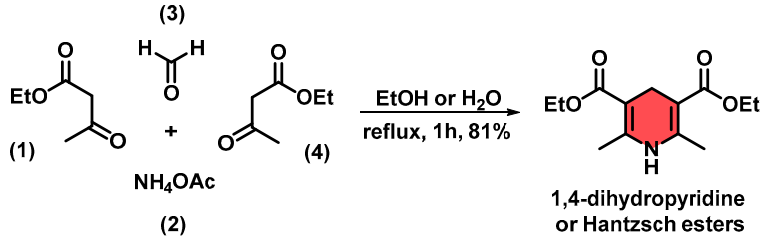

Scheme 2. The Hantzsch synthetic method, a classical 1,4-DHP synthesis.

Mechanistically, however, the process is nuanced: the pathway can also furnish the 1,2-DHP isomer as a competitive side product. Selectivity is governed primarily at the stage of Michael addition of the enamine intermediate to the β-dicarbonyl compound, where two alternative nucleophilic trajectories can lead to either the classical 1,4-DHP or the less common 1,2-isomer (Scheme 3). This duality enriches the reaction's chemical complexity and underscores its usefulness as a model for studying regioselectivity and heterocycle construction [24]. Li Shen et al. systematically demonstrated the exclusive formation of 1,2-dihydropyridine derivatives under catalyst-free, solvent-free Hantzsch-type conditions [25].

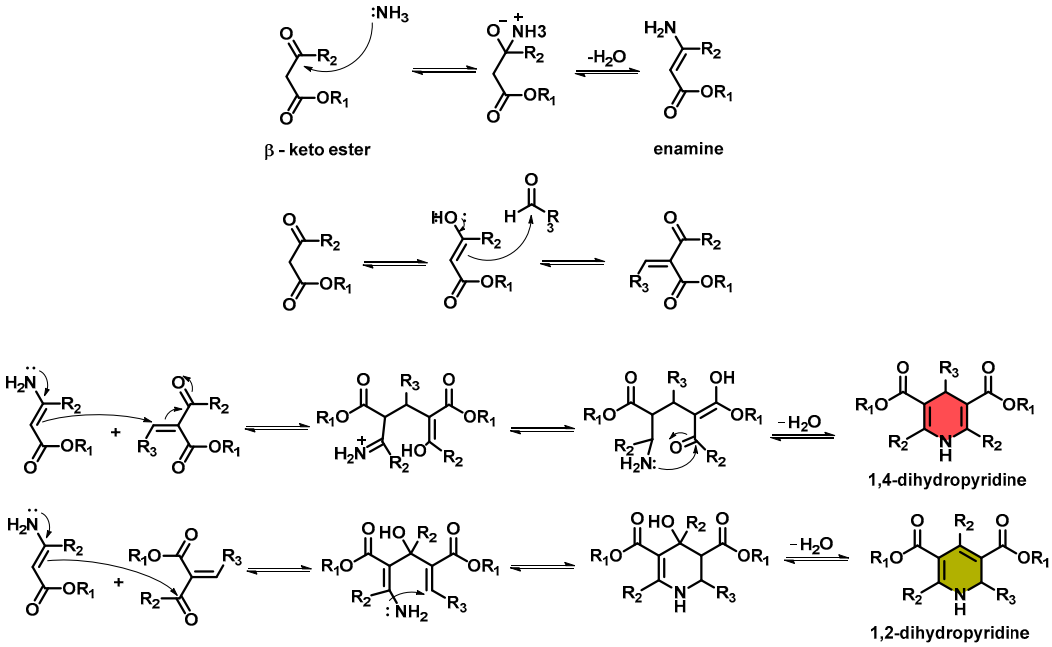

Scheme 3. General mechanism of Hantzsch 1,4-DHP and 1,2-DHP.

Several synthetic strategies have been developed for the preparation of 1,4-DHPs, including microwave-assisted organic synthesis (MAOS), ultrasonic irradiation, green methodologies, ionic liquids, heterogeneous catalysis, and solvent-free conditions [26–33]. Conventionally, 1,4-DHPs have been synthesized under thermal conditions, typically requiring heating at elevated temperatures (80–120 °C) for prolonged reaction times (4–24 h). These protocols often suffer from modest yields, limited regioselectivity with concomitant formation of isomeric mixtures and by-products, as well as excessive energy consumption.

To address these limitations, MAOS combined with heterogeneous catalysis and the use of greener solvents has emerged as an efficient and sustainable alternative [26–29]. This strategy enables precise temperature control and markedly shortens reaction times (typically 1–30 min), while improving product yields and suppressing undesired side

reactions. Overall, these features render MAOS-based protocols fully consistent with the principles of green chemistry.

Over the years, these methodologies have undergone continuous refinement, driven by systematic efforts to expand the scope and performance of available catalytic systems. Although significant progress has been achieved in improving reaction efficiency and product selectivity, challenges related to catalyst recyclability, substrate generality, and operational sustainability remain. In this context, several influential studies reported over the past decade have contributed to advancing the synthesis of 1,4-DHPs through the development of greener catalysts, more sustainable reaction media, and innovative activation strategies, thereby reinforcing—yet not fully exhausting—the principles of modern green chemistry.

In 2018, Chen et al. reported a representative example of solvent-controlled regioselective synthesis of 1,4-DHPs through a cascade multicomponent reaction between enaminones and aldehydes under Brønsted acid catalysis (*p*-TsOH) [34]. In this study, the reaction solvent played a decisive role in directing product formation. Specifically, reactions carried out in ethanol under reflux selectively afforded one class of 1,4-DHP derivatives, whereas replacing ethanol with acetonitrile led to divergent cyclization pathways and the formation of structurally distinct 1,4-DHP frameworks. The transformation proceeds via a cascade sequence involving enaminone activation, an aza-ene reaction, iminium ion formation, and subsequent intramolecular cyclization or elimination steps, enabling the construction of multiple C–C and C–N bonds in a single operation. The methodology operates under relatively mild conditions, exhibits a broad substrate scope encompassing both electron-rich and electron-deficient aldehydes, and clearly demonstrates how subtle variations in reaction parameters—particularly solvent polarity—can significantly influence regioselectivity and overall reaction outcome in Hantzsch-type multicomponent systems, Scheme 4.

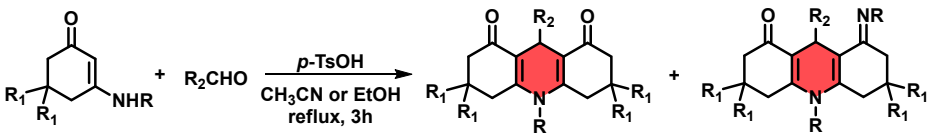

Scheme 4. Solvent-directed regioselective formation of structurally distinct 1,4-DHPs under *p*-TsOH catalysis.

In 2020, Bosica et al., described an efficient route for the synthesis of 1,4-DHPs employing phosphotungstic acid (HPW) heterogenized on alumina (40%) as a reusable solid catalyst. Interestingly, the use of green solvents such as water or ethanol was found to decrease the reaction efficiency, while increasing the temperature had only a minor influence on yield or reaction time. After systematic optimization and evaluation of different heterogeneous catalysts, the authors achieved yields exceeding 75% within just 2–3 h. The optimized alumina-supported catalyst demonstrated excellent reusability, maintaining high activity over eight consecutive reaction cycles and successfully passing the heterogeneity test. Furthermore, substrate scope studies revealed that aliphatic aldehydes furnished the classical 1,4-DHP framework, whereas aromatic aldehydes predominantly afforded the previously reported regioisomeric products (Scheme 5) [35].

Also, in 2020, Tiwari and co-workers reported a green, simple, and efficient one-pot multicomponent Hantzsch synthesis for the preparation of 1,4-DHPs using glycerol as both the reaction medium and promoter. Glycerol exhibited dual functionality—serving as a solvent that effectively dissolves the reactants and as an activator of electrophilic substrates through strong hydrogen-bonding interactions.

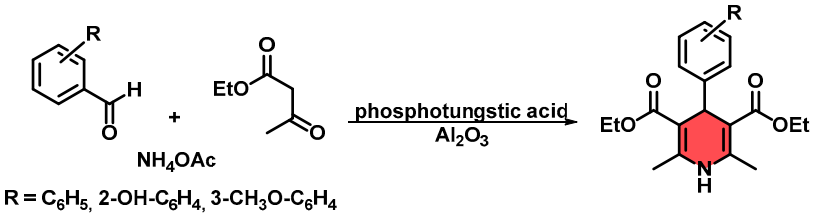

Scheme 5. Synthesis of 1,4-DHPs using phosphotungstic acid, aluminum oxide as catalyst.

In this method, aromatic aldehydes, dimedone, and ammonium acetate were combined with glycerol and heated at 65 °C for a specific duration under mild, metal-free conditions. The process proved to be rapid, cost-effective, and environmentally benign, affording moderate to excellent yields with good atom economy. Due to its simplicity and sustainability, this glycerol-based protocol represents a promising green alternative for the synthesis of 1,4-DHP derivatives with potential physiological activity (Scheme 6) [36].

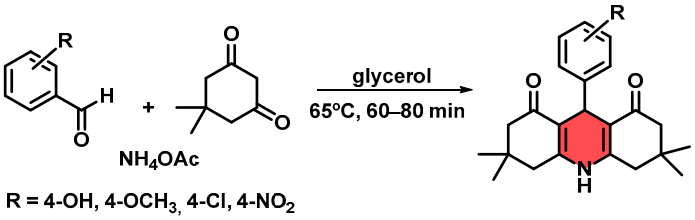

Scheme 6. Synthesis of 1,4-DHPs based using glycerol as catalyst.

A study reported by Jabir et al. in 2020 demonstrated the effectiveness of Brønsted acidic ionic liquids as green catalysts in Hantzsch-type multicomponent reactions, Scheme 7. In this context, a representative example is the one-pot four-component synthesis 1,4-DHPs using 3-methyl-1-sulfonic acid imidazolium chloride ([Msim]Cl) as an efficient and recyclable acidic catalyst. The methodology involves the condensation of aldehydes, β-dicarbonyl compounds, primary amines, and barbituric acid in ethanol under mild conditions, typically at room temperature, affording the desired 1,4-DHP derivatives in high yields and short reaction times. The ionic liquid plays a dual role as both catalyst and reaction medium, enabling effective activation of carbonyl substrates while avoiding the need for harsh reaction conditions [37].

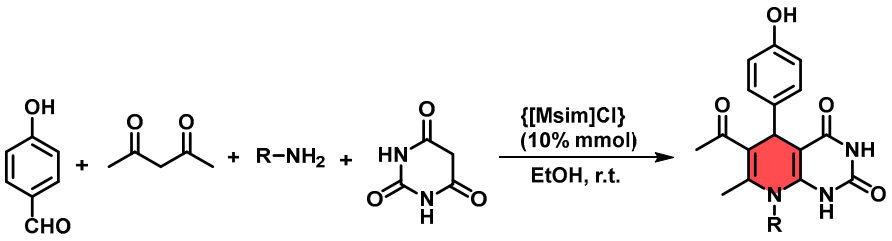

Scheme 7. MCR synthesis of 1,4 DHPs using ionic liquid as catalyst.

Ersatir and co-workers in 2022, reported a simple, environmentally friendly, and highly efficient protocol for the synthesis of 1,4-DHPs. The method involves a one-pot multicomponent reaction (MCR) performed in subcritical ethanol, in which various aromatic aldehydes, ethyl acetoacetate, and urea are converted into the corresponding 1,4-DHP derivatives. The reaction proceeds at 220 °C for 60 min, with its progress conveniently monitored by thin-layer chromatography (TLC). This approach affords good to excellent yields, short reaction times, and straightforward work-up procedures, representing a highly practical and sustainable route for the preparation of 1,4-DHPs. However, the relatively high reaction temperature (220 °C) may limit its application to thermally stable substrates

and increase energy consumption, partially offsetting the environmental advantages of the protocol (Scheme 8) [38].

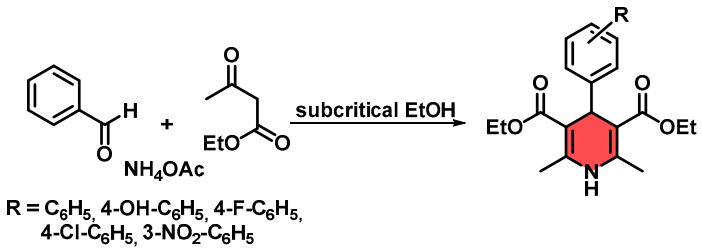

Scheme 8. MCR synthesis of 1,4-DHPs under subcritical ethanol conditions.

In 2024, Pachipulusu and co-workers reported a green and efficient microwave-assisted protocol for the synthesis of 1,4-DHPs. The reaction employed ethanol as a sustainable solvent and triethylamine as a mild base catalyst, enabling the formation of the desired products in less than 30 min with excellent yields (90–96%). This four-component process effectively reduces reagent and solvent consumption, while microwave irradiation enhances both reaction rate and energy efficiency. In addition, the protocol eliminates the need for column chromatography, simplifying product isolation and purification. However, the use of triethylamine, although mild and efficient, introduces a volatile organic base that may slightly compromise the overall greenness of the process and limit its scalability. Despite this limitation, the methodology demonstrates high atom economy, operational simplicity, and short reaction times, representing a sustainable and versatile strategy for the rapid synthesis of heterocyclic scaffolds with potential applications in pharmaceutical and medicinal chemistry (Scheme 9) [39].

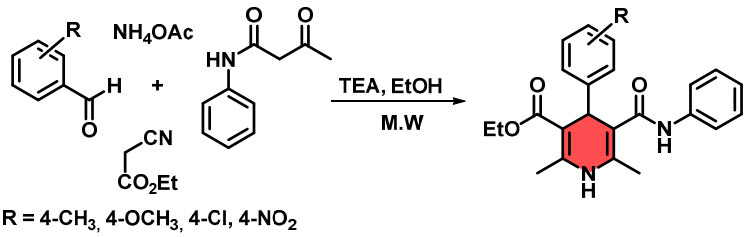

Scheme 9. One-pot multicomponent synthesis of 1,4-DHPs catalyzed by triethylamine (TEA).

Guided by the principles of green chemistry, this study explores a sustainable route for the synthesis of 1,4-DHP derivatives. While conventional Hantzsch protocols typically rely on homogeneous Brønsted acids, organic solvents, prolonged heating, and offer limited control over regioselectivity, recent efforts have shifted toward greener strategies involving alternative reaction media, recyclable heterogeneous catalysts, and energy-efficient activation methods.

In this context, we report the use of a heteropolyacid catalyst, phosphotungstic acid ($H_3PW_{12}O_{40}$, HPW), dissolved in polyethylene glycol (PEG-400) under microwave-assisted conditions. This platform was designed to enhance reaction efficiency by affording higher yields, shorter reaction times, improved regioselectivity toward the 1,4-DHP isomer, and effective catalyst recyclability, while reducing solvent usage and energy consumption.

Accordingly, the present work advances prior methodologies by directly comparing this innovative HPW/PEG-400 microwave-assisted system with a classical thermal approach, systematically optimizing key reaction parameters and demonstrating that sustainability and synthetic performance can be simultaneously achieved.

2. Results and Discussion

To establish a comparative benchmark, the methodology described by Chen et al. was first examined [34]. In their protocol, substituted enaminones and aldehydes are condensed in acetonitrile under reflux in the presence of 30 mol% of the *p*-toluenesulfonic acid (*p*-TsOH), affording 1,4-DHP derivatives in 3 h with moderate yields (Scheme 4).

The procedure was adapted by replacing the previously synthesized enaminone component with its corresponding precursors, ethyl acetoacetate and ammonium formate, which were employed for in situ enaminone generation using the same stoichiometric proportions. Under these modified conditions, the reaction with benzaldehyde afforded two isomeric products—the 1,4-DHP and 1,2-DHP derivatives (Scheme 10)—in contrast to the exclusive formation of the 1,4-DHP reported by Chen et al.

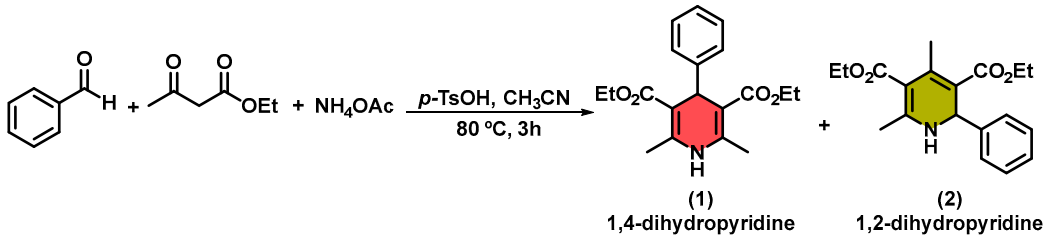

Scheme 10. General procedure adapted from Chen et al. for the synthesis of 1,4-DHPs.

In the study by Cheng et al., the selective formation of the 1,4-DHP isomer may be attributed to conformational constraints that direct the reaction pathway toward this product, thereby suppressing the formation of the 1,2-DHP regioisomer, structural characterization was performed by ^{1}H NMR spectroscopy (see Supporting Information).

Variation in these parameters consistently led to the formation of both regioisomers. Upon recrystallization from ethanol, the 1,4-dihydropyridine scaffold (1) and the 1,2-dihydropyridine scaffold (2) afforded crystals with distinct morphologies, enabling straightforward physical separation in a 1.5:1 ratio, as determined by HPLC (see Supporting Information). Compound **1** was isolated as larger yellow crystals, whereas compound **2** was obtained as smaller white crystals. Single-crystal X-ray diffraction analysis provided unambiguous structural confirmation, and the corresponding ORTEP representations are shown in Figure 5.

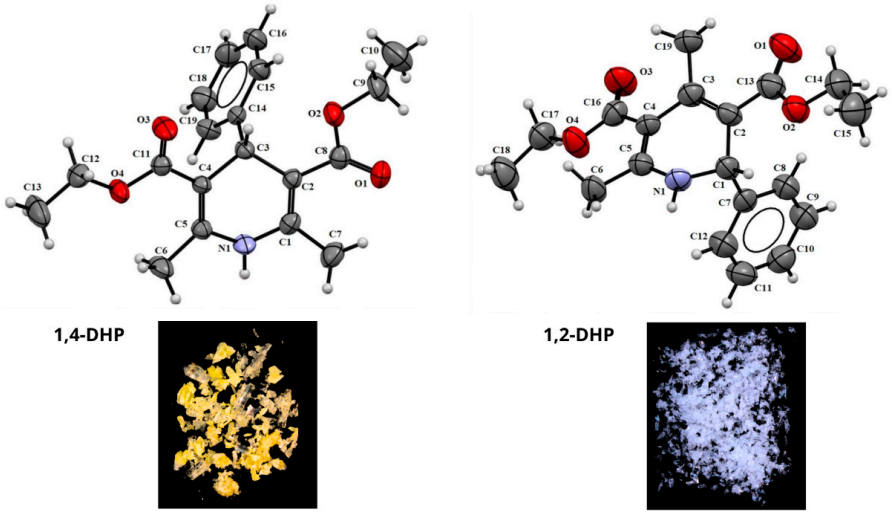

Figure 5. ORTEP representations of the 1,4-DHP and 1,2-DHP isomers from single-crystal X-ray diffraction (50% probability ellipsoids), with photographs of the corresponding crystalline samples shown below each structure, highlighting their distinct solid-state morphology and color.

This unexpected divergence prompted a systematic investigation into the factors governing regioisomer formation, including the effects of catalyst type, reaction time, solvent, and related parameters. Overall, adaptation of the conditions reported by Chen et al. fundamentally altered the reaction outcome, consistently leading to mixtures of the 1,4- and 1,2-DHP isomers. Accordingly, we expanded the exploration of this methodology to examine regioisomer formation and to enable a robust and meaningful comparison between our methodology and that of Chen et al., as well as the adapted protocol, as summarized in Table 1.

Table 1. Substrate scope expansion of the *p*-TsOH/acetonitrile system under conventional heating, showing isolated yields and 1,4-DHP/1,2-DHP regioselectivity.

Entry	R	Ratio 1,4-DHP:1,2-DHP [a]	Yield% [b]
1	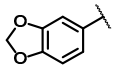	1.1:1	9
2	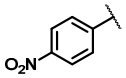	2:1	15
3	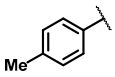	2:1	11
4	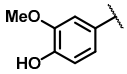	1.2:1	13
5	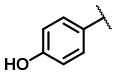	2:1	10
6	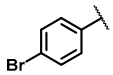	4:1	21
7	H	2:1	30

[a] The ratio was determined from HPLC peak areas. [b] Yield of the regioisomeric mixture comprising compounds **1** and **2**.

The products could not be purified, even after column chromatography followed by recrystallization. Consequently, isolated yields were determined for the regioisomeric mixtures, and regioselectivity was assessed by HPLC (see Supplementary Materials). Overall, the yields were very low (9–40%), in good agreement with the low yields previously reported by Chen et al. In some cases (entries 1 and 4), the reaction afforded an almost equimolar mixture of regioisomers, indicating negligible regioselectivity. This poor regioselectivity demonstrates that the reaction system does not efficiently promote selective formation of the thermodynamically preferred product, suggesting competition between the two mechanistic pathways outlined in Scheme 3.

The regioselective formation of 1,2-DHPs, in contrast to the more commonly observed 1,4-DHPs, can be rationalized by deviations from the classical Hantzsch reaction mechanism. In particular, differences in nucleophile hardness—arising from electronic effects of substituents on the aldehyde—and the nature of the reactive intermediates can influence the site of nucleophilic addition, occasionally favoring 1,2-addition pathways. When the reaction mechanism diverges from the canonical enamine–Knoevenagel–Michael addition sequence—such as through the involvement of alternative enamine intermediates or direct nucleophilic attack—formation of 1,2-DHPs becomes potentially accessible. Under typical multicomponent condensation conditions involving an aldehyde, two β-keto esters, and ammonia or amines, however, the pathway leading to 1,4-DHPs remains both kinetically

and mechanistically preferred. This intrinsic bias accounts for why the vast majority of reported methodologies, including those employing acid catalysis, diverse solvent systems, or microwave irradiation, predominantly afford the 1,4-DHP regioisomer.

In order to ensure a comprehensive study and generate reliable, directly comparable data, the reaction was also evaluated under the same conditions by replacing the acetonitrile *p*-TsOH system with the HPW/PEG-400 catalytic system, Scheme 11.

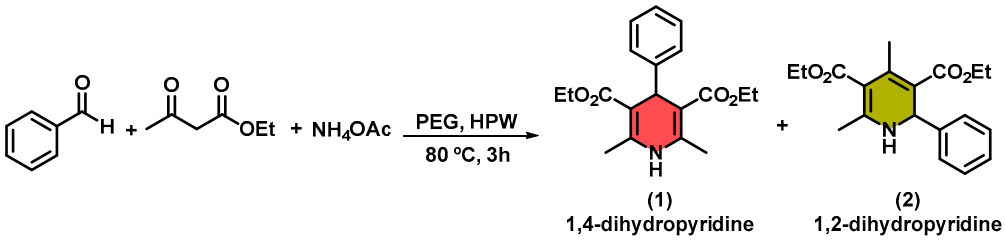

Scheme 11. Evaluation of the reaction under identical conditions using the HPW/PEG-400 catalytic system as a replacement for the acetonitrile/*p*-TsOH system.

Overall, the results revealed a significant increase in yield (52%) and, notably, a substantial enhancement in regioselectivity (1,4-DHP/1,2-DHP = 22:1), indicating that the HPW/PEG-400 system is more efficient in promoting formation of the 1,4-DHP scaffold when compared with the acetonitrile/*p*-TsOH system, (see Supporting Information).

Building on our continued interest in MAOS [40] and in light of the results obtained under the previously reported adapted conditions, we initiated our investigations using a microwave-assisted methodology based on an HPW catalytic system in PEG-400. To evaluate the optimal catalyst loading, a fixed reaction time of 30 min was established for this stage, and the catalyst amount was systematically varied as summarized in Table 2.

Table 2. Optimization of HPW catalyst loading in PEG-400 under microwave irradiation using a fixed reaction time of 30 min.

Entry	mol% Catalyst	Ratio (1,4-DHP:1,2-DHP) [a]	Yield (%)
1	30	35:1	72
2	20	35:1	74
3	10	38:1	75
4	5	38:1	75
5	1	8:1	47

[a] The ratio was determined from HPLC peak areas.

As summarized in Table 2, the HPW/PEG-400 catalytic system exhibits high robustness across a broad range of catalyst loadings. When 30–5 mol% HPW was employed (entries 1–4), both the isolated yields and the 1,4-DHP/1,2-DHP ratios remained essentially unchanged, indicating that enamine formation and the subsequent Michael addition are efficiently promoted even at reduced catalyst levels. In contrast, at 1 mol% HPW (entry 5), corresponding to a 30- to 5-fold lower catalyst loading relative to the preceding conditions, a marked decrease in both yield and regioselectivity was observed. To further assess the influence of reaction time under such low catalyst loading, the conditions used in entry 5 were extended to 60 min. No significant changes in either regioselectivity or yield were observed, indicating that longer reaction times do not compensate for the reduced density of acidic sites. Taken together, these observations support the existence of a catalytic threshold below which the HPW/PEG-400 system cannot efficiently sustain the classical Hantzsch pathway, regardless of reaction time.

Building on these results, the effects of reaction time and temperature were subsequently examined to determine the optimal reaction conditions (Table 3).

Table 3. Optimization of reaction time and temperature to establish the most efficient conditions.

Entry	Time (min.)	Solvent	Catalyst	Temp. (°C)	Ratio (1,4-DHP:1,2-DHP) [a]	Yield (%)
1	10	PEG-400	HPW	80	33:1	71
2	20	PEG-400	HPW	80	38:1	80
3	30	PEG-400	HPW	80	33:1	75
4	40	PEG-400	HPW	80	33:1	53
5	60	PEG-400	HPW	80	33:1	51
6	20	Solvent-free	HPW	80	-	-
7	20	PEG-400	Catalyst-free	80	-	-
8	20	PEG-400	HPW	60	20:1	60
9	20	PEG-400	HPW	100	55:1	52
10	10	PEG-400	HPW	150	40:1	45

[a] The ratio was determined from HPLC peak areas.

Entries 1–5 highlight the critical role of reaction time on yield, as the regioisomeric ratios remain relatively constant and significantly higher than those obtained using the adapted methodology under conventional heating. In entries 3, 4 and 5, a decrease in yield was observed, likely due to degradation and oxidation of the reagents promoted by prolonged reaction times and elevated temperatures. Entry 2 provided the most favorable outcome, affording an 80% yield with a 1,4-DHP/1,2-DHP ratio of 33:1 (see Supporting Information). Entries 6 and 7 demonstrate that the reaction is strongly dependent on both the solvent and the catalytic system, as no product formation was detected in their absence. Based on the robust results obtained in entry 2, we subsequently investigated the effect of temperature. Owing to the sealed nature of the microwave system, which allows reactions to be conducted at temperatures above the boiling point of the corresponding solvents, a temperature study was feasible. As observed in entry 8, lower temperatures led to decreased yield and reduced regioisomeric selectivity. In contrast, entry 9 shows that higher temperatures significantly increased the regioisomeric ratio; however, the overall yield decreased due to the onset of reagent degradation. A comparable trend was observed in entry 10, where reducing the reaction time while increasing the temperature still resulted in an unsatisfactory overall yield, indicating a pronounced temperature effect on product formation. A substantial loss in regioselectivity was also detected under these conditions, demonstrating that elevated temperatures negatively impact both the efficiency and selectivity of the process.

To complete the comparative evaluation between the methodologies, the reaction was also investigated using the acetonitrile *p*-TsOH system under microwave-assisted conditions at 80 °C for 20 min, Scheme 12.

The results are particularly noteworthy when compared with conventional thermal heating. Under microwave irradiation, the reaction yield increased from 40% to 58%, accompanied by a pronounced enhancement in regioselectivity from 1.5:1 to 24:1, highlighting the significant influence of both exposure time and heating mode. The effect of microwave irradiation on the organization of the solvation layer may enhance the catalytic activity of *p*-TsOH; however, across all conditions investigated, our methodology consistently outperformed the acetonitrile/*p*-TsOH system. These findings underscore the synergistic

role of the HPW/PEG-400 catalytic system combined with microwave-assisted heating in achieving superior efficiency and selectivity.

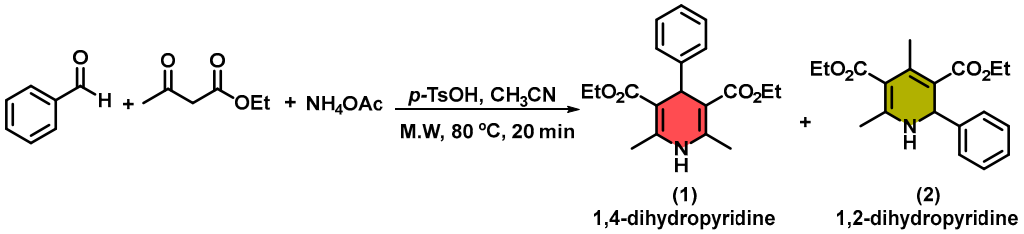

Scheme 12. Evaluation of the acetonitrile/*p*-TsOH system under microwave-assisted conditions (80 °C, 20 min) for comparative purposes.

With the optimal reaction conditions established for this system, we proceeded to the synthesis of a series of 1,4-DHP derivatives using the same aliphatic and aromatic aldehydes employed in the initial studies, in which the methodology of Cheng et al., had been adapted, while maintaining all other reagents consistent with those used in the preceding stages of this work. The reaction conditions adopted correspond to those defined in entry 2 of Table 2, namely a reaction time of 20 min under microwave irradiation at 80 °C, using HPW as the catalyst and PEG-400 as the solvent, Scheme 13.

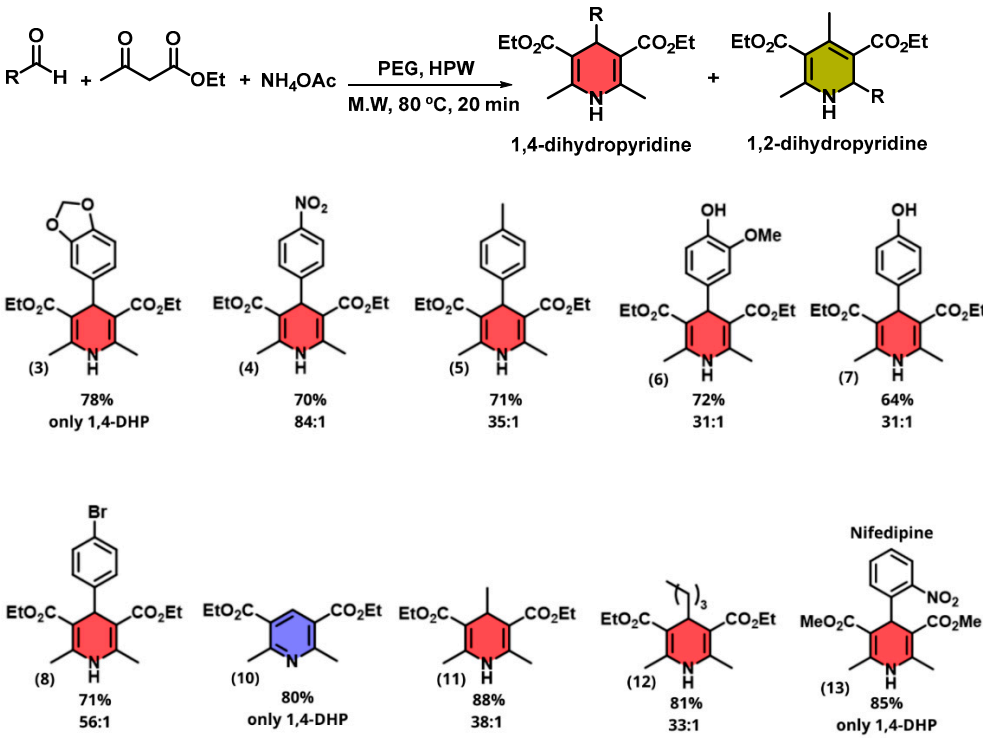

Scheme 13. Scope of the microwave-assisted HPW/PEG-400 methodology using various aldehydes, showing isolated yields and 1,4-DHP/1,2-DHP regioselectivity.

Overall, the yields obtained under these conditions were significantly higher than those achieved with the reference methodology, both in terms of overall efficiency and regioisomer distribution. Although minor amounts of 1,2-DHP derivatives were consistently detected, the regioselectivity toward the 1,4-DHP isomer was sufficiently high that the 1,2-DHP could not be reliably quantified by NMR spectroscopy. This observation may explain why relatively few studies report the isolation of this regioisomer, often describing it merely as an impurity. Taken together, these results indicate that the transformation proceeds through the classical Hantzsch mechanism, which kinetically and thermodynamically favors 1,4-DHP formation via the enamine–Knoevenagel–Michael sequence.

To further investigate the influence of the aldehyde component on regioselectivity, the methodology was applied to two aliphatic aldehydes to evaluate potential shifts in the 1,4- vs. 1,2-DHP distribution, as previously noted by Bosica et al. for related systems [35]. In both cases, the desired 1,4-DHP derivatives were obtained in good yields and with high regioselectivity, thereby reinforcing the robustness of the present protocol.

Finally, to demonstrate synthetic applicability, the methodology was employed for the preparation of nifedipine, a clinically relevant calcium channel blocker. The target compound was obtained in high yield and with excellent regioselectivity, further underscoring the practical value of the HPW/PEG-400 microwave-assisted system.

Another important aspect to be considered is the potential stabilization of reaction intermediates and transition states by the PEG-400 solvent through hydrogen-bonding interactions, as well as the formation of aggregation clusters with HPW that may further enhance its acidic character. This behavior may account for the outcome observed in Scheme 14, in which the reaction employing paraformaldehyde—a more stable and less reactive form of formaldehyde—led to the formation of the corresponding pyridine as the final product. Following initial formation of the 1,4-DHP intermediate, the strongly acidic reaction medium may promote dehydrogenation of the dihydropyridine core, ultimately leading to aromatization of the ring system [41].

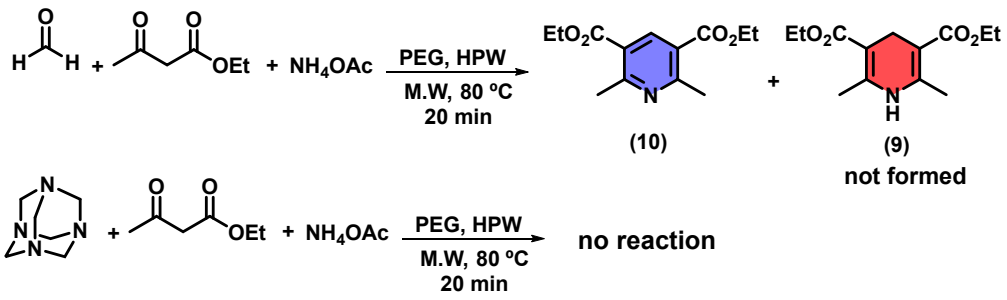

Scheme 14. Influence of the formaldehyde source under strongly acidic conditions: paraformaldehyde leads to pyridine formation via 1,4-DHP aromatization, whereas hexamethylenetetramine (HMTA) is unreactive.

In an attempt to obtain product 9, hexamethylenetetramine (HMTA) was evaluated as an alternative formaldehyde source; however, no reaction was observed, Scheme 14. A plausible explanation is that formaldehyde generated in situ from HMTA undergoes rapid oxidation to its corresponding acidic form under the strongly acidic conditions, thereby preventing its participation in the desired condensation pathway and precluding formation of the targeted product.

The recyclability of the HPW/PEG-400 catalytic system was also evaluated. After completion of the reaction, an organic solvent was added and the mixture was vigorously stirred. After a settling period, the system was cooled to −20 °C to promote phase separation. The organic phase containing the reaction products from benzaldehyde, ethyl acetoacetate, and ammonium acetate was carefully removed using a pipette. The remaining HPW/PEG-400 phase was concentrated under reduced pressure, dried under high vacuum, and subsequently reused. The recovered catalytic system was successfully reused for five consecutive cycles without significant variations in either yield or regioselectivity (33:1, Figure 6). A noticeable decrease in yield was only observed in the sixth cycle, which we attribute to partial catalyst deactivation and the gradual accumulation of impurities from previous reactions in the PEG-400 phase. Attempts to characterize these impurities by NMR were unsuccessful. No significant change in regioselectivity was detected even at this stage. Accordingly, we report five cycles as a practical and safe operational limit for the HPW/PEG-400 system.

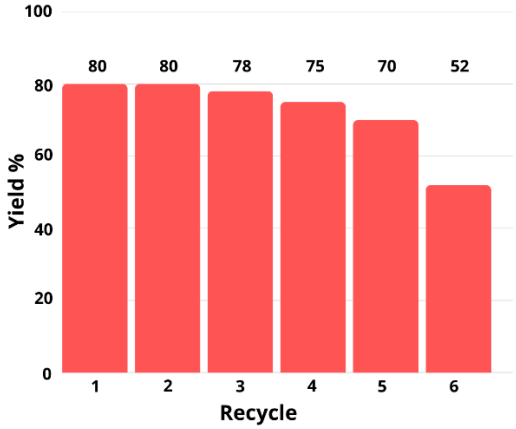

Figure 6. Recycling and reuse of the HPW/PEG-400 catalytic system in the synthesis of 1,4-DHPs.

3. Materials and Methods

All reagents and solvents were purchased from Sigma-Aldrich-Merck (St. Louis, MO, USA), and used as received. Commercial reagents exhibited analytical-grade purity suitable for synthetic organic chemistry. Microwave reactions were performed using a Biotage Initiator+ (Biotage, Uppsala, Sweden) microwave reactor equipped with sealed vessels, a dynamic power control program, simultaneous cooling, media stirring, and real-time temperature monitoring by an internal fiber-optic probe. The Biotage Initiator+ system operates at a fixed microwave frequency of 2.45 GHz with an automated power range of 0–400 W. The NMR spectra were recorded at 25 °C on a Bruker Avance 600 spectrometer (Bruker, Billerica, MA, USA, 600 MHz for ^{1}H and 151 MHz for ^{13}C) with TMS as an internal standard for deuterated chloroform ($CDCl_3$) as solvent. The reactions were monitored by thin-layer chromatography (TLC) on precoated 0.25 mm thick plates of Kieselgel 60 F_{254} (Merck, Burlington, MA, USA), visualization was accomplished by UV light (254 nm) or by spraying a solution of 10% solution of phosphomolybdic acid in ethanol, followed by heating at 200 °C for a sufficient duration until blue spots become visible. HRESI-MS (ESI-QTOF) experiments were performed on a Triple Tof 5600 Sciex (SCIEX, Framingham, MA, USA), by flow injection analysis using an Eksigent UltraLC 100 Sciex chromatograph set to a flow rate of 0.3 mL/min. All melting points were measured using capillary tubes on a LOGEN Scientific -LS III Plus (Diadema, São Paulo, Brazil) melting point apparatus. High-performance liquid chromatography (HPLC) analyses were performed on an Agilent Technologies 1100 Series system (Agilent Technologies, Inc., headquartered in Santa Clara, CA, USA). The analytical separations were carried out using a Kinetex C18 column (5 µm, 250 × 4.6 mm) under isocratic conditions with water/acetonitrile (60:40, *v*/*v*) as the mobile phase. The X-ray diffraction data were collected at room temperature (296 K) on a Bruker CCD SMART APEX II (Bruker Corporation, Billerica, MA, USA), single crystal diffractometer with Mo Kα radiation (0.71073 Å). The structures were solved using the Olex2 program [42] by direct methods with SHELXS [43], and subsequent Fourier-difference map analyses yielded the positions of the non-hydrogen atoms. The refinement was performed using SHELXL [44]. Empirical absorption corrections were applied using the SADABS program [45]. Full-matrix least-squares made all refinements on F2 with anisotropic displacement parameters for all non-hydrogen atoms. Hydrogen atoms were included in the refinement in calculated positions, but the atoms (of hydrogens) that are commenting performing special bonds were located in the Fourier map. Molecular graphics were generated via MERCURY 4.0 software [46]. Crystallographic data for the structures in this work were deposited at the Cambridge Crystallographic Data Centre,

CCDC-2517790 and CCDC-2517791. Crystal data, experimental details, and refinement results are summarized in Table S1.

3.1. General Synthesis of 1,4-Dihydropyridines in Acetonitrile Using TsOH

In a 50 mL round-bottom flask, an aldehyde (5 mmol), ethyl acetoacetate (10 mmol), ammonium acetate (10 mmol), and p-toluenesulfonic acid (p-TsOH, 0.3 mmol) were dissolved in acetonitrile (10 mL) and refluxed for 3 h. The reaction progress was monitored by TLC (silica gel, CH_2Cl_2/EtOAc, 9:1, v/v). After completion, the reaction mixture was extracted three times with ethyl acetate and water. The combined organic layers were dried over anhydrous Na_2SO_4, filtered, and concentrated under reduced pressure. The resulting crude product was purified by silica gel column chromatography (CH_2Cl_2/EtOAc, 95:5 → 90:10, v/v) and subsequently recrystallized from ethanol to afford the desired product.

3.2. General Synthesis of 1,4-Synthesis in PEG-400 Using HPW

In a 50 mL round-bottom flask, benzaldehyde (5 mmol), ethyl acetoacetate (10 mmol), ammonium acetate (10 mmol), and phosphotungstic acid (HPW, 0.3 mmol) were dissolved in PEG-400 (10 mL) and heated at 80 °C for 3 h. The reaction progress was monitored by TLC (silica gel, CH_2Cl_2/EtOAc, 9:1, v/v). After completion, the reaction mixture was extracted three times with ethyl acetate and water. The combined organic layers were dried over anhydrous Na_2SO_4, filtered, and concentrated under reduced pressure. The resulting crude product was purified by silica gel column chromatography (CH_2Cl_2/EtOAc, 95:5 → 90:10, v/v) and subsequently recrystallized from ethanol to afford the desired product.

3.3. General Microwave-Assisted Synthesis of 1,4-Dihydropyridines in Acetonitrile Using TsOH

Under optimized conditions, benzaldehyde (1 mmol), ethyl acetoacetate (2 mmol), ammonium acetate (2 mmol), and TsOH (0.05 mmol) were dissolved in acetonitrile (2.5 mL) in a sealed 10 mL glass tube and irradiated at 80 °C for 20 min. After cooling to room temperature, the mixture was partitioned between ethyl acetate and water. The organic layer was dried over anhydrous Na_2SO_4, filtered, and concentrated under reduced pressure. The crude product was purified by silica gel column chromatography (CH_2Cl_2/EtOAc 95:5 → 90:10) and recrystallized from ethanol to afford the desired product.

3.4. General Microwave-Assisted Synthesis of 1,4-Dihydropyridines in PEG-400 Using HPW

Under optimized conditions, aldehyde (1 mmol), ethyl acetoacetate (2 mmol), ammonium acetate (2 mmol), and HPW (5 mol%, 0.05 mmol) were dissolved in PEG-400 (1.5 mL) in a sealed 10 mL glass tube and irradiated in a Biotage Initiator+ microwave reactor (80 °C, 20 min) under magnetic stirring. After cooling to room temperature, the product was extracted with diethyl ether (3 × 5 mL) by decantation. For PEG-400 systems, the mixture was cooled to solidify the PEG phase, enabling separation of the ether extract. The combined organic layers were dried over anhydrous Na_2SO_4, filtered, concentrated under reduced pressure, purified by silica gel column chromatography (CH_2Cl_2/EtOAc 95:5 → 90:10), and recrystallized from ethanol to afford the desired product.

The isolated solid 1,4-DHP derivatives were characterized by ^{1}H NMR, ^{13}C NMR, HRMS (ESI-TOF), and melting point analysis. The analytical data were consistent with previously reported values.

Diethyl 2,6-dimethyl-4-phenyl-1,4-dihydropyridine-3,5-dicarboxylate (1) [38]:

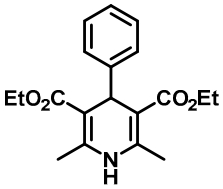

^{1}H NMR (600 MHz, $CDCl_3$) δ 7.27 (d, *J* = 7.70 Hz, 2H), 7.20 (t, *J* = 7.66 Hz, 2H), 7.12 (t, *J* = 7.50 Hz, 1H), 5.78 (s, 1H), 4.99 (s, 1H), 4.04–4.13 (m, 4H), 2.31 (s, 6H), 1.22 (t, J = 7.11 Hz, 6H). ^{13}C NMR (151 MHz, $CDCl_3$) δ 167.7, 147.8, 143.9, 128.0, 127.8, 126.1, 104.1, 59.7, 39.6, 19.5, 14.2. HRMS (ESI-TOF) *m*/*z* calculated for $C_{19}H_{24}NO_4^+$ $[M + H]^+$: 330.1627; found $[M + H]^+$: 330.1626. mp: 155–157 °C (yellow solid).

Diethyl 2,4-dimethyl-6-phenyl-1,4-dihydropyridine-3,5-dicarboxylate (2) [35]:

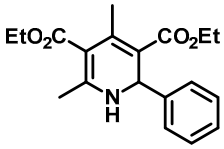

^{1}H NMR (600 MHz, $CDCl_3$) δ 7.24–7.30 (m, 5H), 5.61 (d, *J* = 4.05 Hz, 1H), 5.41 (d, *J* = 4.05 Hz, 1H), 4.08–4.25 (m, 2H), 2.39 (s, 3H), 2.22 (s, 3H), 1.30 (t, *J* = 7.13 Hz, 3H), 1.21 (t, *J* = 7.13 Hz, 3H). ^{13}C NMR (151 MHz, $CDCl_3$). HRMS (ESI-TOF) *m*/*z* calculated for $C_{19}H_{24}NO_4^+$ $[M + H]^+$: 330.1627; found $[M + H]^+$: 330.1626. mp: 145–146 °C (white solid).

Diethyl 4-(benzo[1,3]dioxol-5-yl)-2,6-dimethyl-1,4-dihydropyridine-3,5-dicarboxylate (3) [47]:

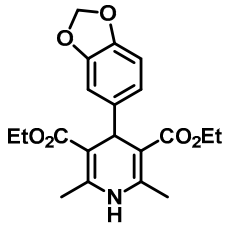

^{1}H NMR (600 MHz, $CDCl_3$) δ 6.78 (d, J = 1.65 Hz, 1H), 6.75 (dd, *J* = 8.00, 1.65 Hz, 1H), 6.65 (d, *J* = 7.99 Hz, 1H), 5.87 (s, 2H), 5.73 (s, 1H), 4.92 (s, 1H), 4.06–4.15 (m, 4H), 2.31 (s, 6H), 1.24 (t, *J* = 7.12 Hz, 6H). ^{13}C NMR (151 MHz, $CDCl_3$) δ 167.6, 147.2, 145.7, 143.7, 142.0, 120.9, 108.6, 107.5, 104.3, 100.6, 59.7, 39.3, 19.6, 14.3. HRMS (ESI-TOF) *m*/*z* calculated for $C_{20}H_{24}NO_6$+ $[M + H]^+$: 374.1525; found $[M + H]^+$: 374.1526. mp: 198–200 °C (yellow solid).

Diethyl 2,6-dimethyl-4-(4-nitrophenyl)-1,4-dihydropyridine-3,5-dicarboxylate (4) [38]:

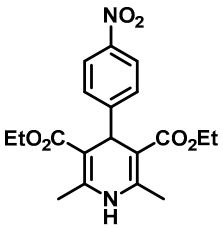

^{1}H NMR (600 MHz, $CDCl_3$) δ 8.10 (d, *J* = 8.80 Hz, 2H), 7.47 (d, *J* = 8.90 Hz, 2H), 5.78 (s, 1H), 5.11 (s, 1H), 4.07–4.15 (m, 4H), 2.38 (s, 6H), 1.24 (t, *J* = 7.12 Hz, 6H). ^{13}C NMR (151 MHz, $CDCl_3$) δ 167.0, 155.1, 146.4, 144.6, 128.9, 123.3, 103.2, 60.0, 40.1, 19.7, 14.3. HRMS (ESI-QTOF) *m*/*z* calculated for $C_{19}H_{23}N_2O_6^+$ $[M + H]^+$: 375.1478; found $[M + H]^+$: 375.1477. mp: 194–196 °C (yellow solid).

Diethyl 2,6-dimethyl-4-(p-tolyl)-1,4-dihydropyridine-3,5-dicarboxylate (5) [38]:

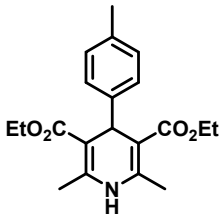

^{1}H NMR (600 MHz, $CDCl_3$) δ 7.19 (d, *J* = 7.87 Hz, 2H), 7.03 (d, *J* = 7.85 Hz, 2H), 5.78 (s, 1H), 4.97 (s, 1H), 4.08–4.15 (m, 4H), 2.34 (s, 6H), 2.29 (s, 3H), 1.25 (t, *J* = 7.14 Hz, 6H). ^{13}C NMR (151 MHz, $CDCl_3$) δ 167.7, 144.9, 143.8, 135.5, 128.6, 127.8, 127.7, 104.2, 60.4, 59.7, 39.1, 21.0, 19.6, 14.3. HRMS (ESI-QTOF) *m*/*z* calculated for $C_{20}H_{26}NO_4^+$ $[M + H]^+$: 344.1784; found $[M + H]^+$: 344.1784. (Yellow pasty solid).

Diethyl 4-(4-hydroxy-3-methoxyphenyl)-2,6-dimethyl-1,4-dihydropyridine-3,5-dicarboxylate (6) [48]:

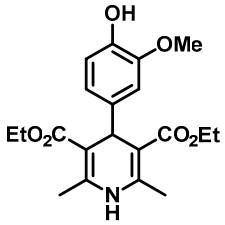

^{1}H NMR (600 MHz, $CDCl_3$) δ 6.95 (d, *J* = 8.31 Hz, 1H), 6.87 (d, *J* = 1.72 Hz, 1H), 6.75 (dd, *J* = 8.30, 1.72 Hz, 1H), 5.69 (s, 1H), 5.50 (s, 1H), 4.94 (s, 1H), 4.09–4.16 (m, 4H), 3.86 (s, 3H), 2.35 (s, 6H), 1.26 (t, *J* = 7.11 Hz, 6H). ^{13}C NMR (151 MHz, $CDCl_3$) δ 167.7, 145.8, 143.9, 143.6, 140.1, 120.5, 113.9, 110.9, 104.3, 59.7, 55.8, 39.1, 19.6, 14.3. $C_{20}H_{26}NO_6^+$ $[M + H]^+$: 376.1682; found $[M + H]^+$: 376.1682. mp: 161–163 °C (yellow solid).

Diethyl 4-(4-hydroxyphenyl)-2,6-dimethyl-1,4-dihydropyridine-3,5-dicarboxylate (7) [38]:

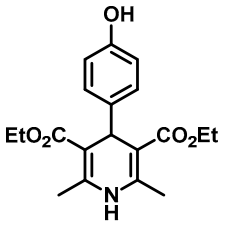

^{1}H NMR (600 MHz, $CDCl_3$) δ 7.15 (d, *J* = 8.39 Hz, 2H), 6.68 (d, *J* = 8.44 Hz, 2H), 5.62 (s, 1H), 4.94 (s, 1H), 4.08–4.17 (m, 4H), 2.34 (s, 6H), 1.24 (t, *J* = 7.11 Hz, 6H). ^{13}C NMR (151 MHz, $CDCl_3$) δ 167.9, 154.0, 143.6, 140.2, 129.2, 114.7, 104.5, 59.8, 38.8, 19.6, 14.3. $C_{19}H_{24}NO_5^+$ $[M + H]^+$: 346.1576 found $[M + H]^+$: 346.1576. mp: 238–240 °C (yellow solid).

Diethyl 4-(4-bromophenyl)-2,6-dimethyl-1,4-dihydropyridine-3,5-dicarboxylate (8) [38]:

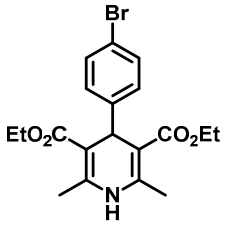

^{1}H NMR (600 MHz, $CDCl_3$) δ 7.34 (d, *J* = 8.40 Hz, 2H), 7.18 (d, *J* = 8.42 Hz, 2H), 5.80 (s, 1H), 4.97 (s, 1H), 4.07–4.14 (m, 4H), 2.34 (s, 6H), 1.24 (t, *J* = 7.12 Hz, 6H). ^{13}C NMR (151 MHz, $CDCl_3$) δ 167.4, 146.9, 143.6, 144.1, 130.9, 129.9, 119.9, 103.8, 59.8, 39.3, 19.6, 14.3. HRMS (ESI-QTOF) *m*/*z* calculated for $C_{19}H_{23}BrNO_4^+$ $[M + H]^+$: 408.0732; found $[M + H]^+$: 408.0734. mp: 241–243 °C (orange solid).

Diethyl 2,6-dimethyl-1,4-dihydropyridine-3,5-dicarboxylate (9) [41]:

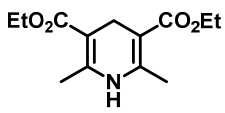

^{1}H NMR (600 MHz, $CDCl_3$) δ 4.16 (q, *J* = 7.12 Hz, 4H), 3.26 (s, 2H), 2.19 (s, 3H), 1.28 (t, *J* = 7.14 Hz, 6H). ^{13}C NMR (151 MHz, $CDCl_3$) δ 168.1, 144.9, 99.5, 59.7, 24.8, 19.2, 14.5. HRMS (ESI-QTOF) *m*/*z* calculated for $C_{13}H_{20}NO_4^+$ $[M + H]^+$: 254.1314; found $[M + H]^+$: 254.1313. mp: 179–182 °C (yellow solid).

Diethyl 2,6-dimethylpyridine-3,5-dicarboxylate (10) [41]:

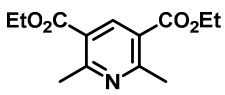

^{1}H NMR (600 MHz, $CDCl_3$) δ 8.70 (s, 1H), 4.41 (q, *J* = 7.14 Hz, 4H), 2.87 (s, 6H), 1.43 (t, *J* = 7.16 Hz, 6H). ^{13}C NMR (151 MHz, $CDCl_3$) δ 165.9, 162.2, 140.9, 123.1, 61.4, 24.9, 14.3. HRMS (ESI-QTOF) *m*/*z* calculated for $C_{13}H_{18}NO_4^+$ $[M + H]^+$: 252.1158; found $[M + H]^+$: 252.1159. mp: 70–73 °C (yellow solid).

Diethyl 2,4,6-trimethyl-1,4-dihydropyridine-3,5-dicarboxylate (11) [49]:

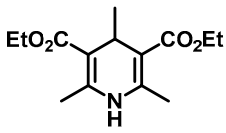

^{1}H NMR (600 MHz, $CDCl_3$) δ 4.67 (m, 4H), 3.74 (q, *J* = 7.14 Hz, 1H), 2.08 (s, 6H), 1.57 (t, *J* = 7.12 Hz, 6H), 0.91 (d, *J* = 4.8 Hz, 3H). ^{13}C NMR (151 MHz, $CDCl_3$) δ 167.6, 147.7, 104.1, 59.7, 27.6, 23.4, 19.5, 14.2. HRMS (ESI-QTOF) *m*/*z* calculated for $C_{14}H_{22}NO_4^+$ $[M + H]^+$: 268.1471; found $[M + H]^+$: 268.1470. mp: 131–132 °C (yellow solid).

Diethyl 4-isobutyl-2,6-dimethyl-1,4-dihydropyridine-3,5-dicarboxylate (12):

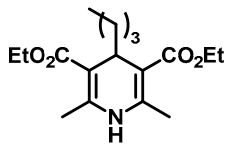

^{1}H NMR (600 MHz, $CDCl_3$) δ 4.17 (q, *J* = 7.15 Hz, 4H), 3.24 (t, *J* = 7.11 Hz, 1H), 2.19 (s, 6H), 1.60-1.57 (m, 6H), 1.55-1.40 (m, 6H), 1.38 (t, *J* = 7.14 Hz, 3H). ^{13}C NMR (151 MHz, $CDCl_3$) δ 168.1, 144.9, 99.5, 59.7, 36.3,32.1, 27.3, 24.8, 19.2, 14.5. HRMS (ESI-QTOF) *m*/*z* calculated for $C_{17}H_{26}NO_4^+$ $[M + H]^+$: 308.1784; found $[M + H]^+$: 308.1783. mp: 155–157 °C (yellow solid).

Dimethyl 2,6-dimethyl-4-(2-nitrophenyl)-1,4-dihydropyridine-3,5-dicarboxylate-Nifedipine (13) [41]:

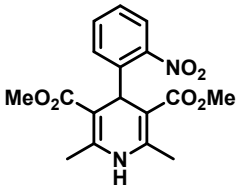

^{1}H NMR (600 MHz, $CDCl_3$) δ 7.85 (d, *J* = 8.0 Hz, 1H), 7.78-7.62 (m, 3H), 5.77 (s,1H), 5.09 (s, 1H), 3.69 (s, 6H); 2.35 (s, 6H). ^{13}C NMR (151 MHz, $CDCl_3$) δ 167.1, 146.4, 144.6, 141.0, 133.4, 130.1, 128.9, 123.3, 103.2, 60.0, 40.1, 19.70 HRMS (ESI-QTOF) *m*/*z* calculated for $C_{13}H_{18}NO_4^+$ $[M + H]^+$: 347.1165; found $[M + H]^+$: 347.1165. mp: 171–173 °C (yellow solid).

4. Conclusions

In summary, this work presents an efficient and environmentally friendly microwave-assisted organic synthesis (MAOS) Hantzsch protocol for the selective synthesis of 1,4-DHPs using a recyclable HPW/PEG-400 catalytic system. Systematic comparison with a classical methodology demonstrates that subtle variations in catalyst–solvent combinations and energy input exert a decisive influence on regioisomer formation, enabling control over the 1,4-DHP/1,2-DHP ratio. Under optimized microwave conditions, the HPW/PEG-400 system consistently favors formation of the kinetically and thermodynamically preferred 1,4-DHP scaffold, affording higher yields, significantly reduced reaction times, and superior regioselectivity relative to conventional thermal protocols. Mechanistic considerations support a classical Hantzsch pathway dominated by the enamine–Knoevenagel–Michael addition sequence, while deviations observed under strongly acidic or solvent-dependent conditions account for competitive 1,2-DHP formation or aromatization events. Moreover, the heterogeneous nature of the PEG/HPW medium enables straightforward catalyst recovery and reuse over multiple cycles with minimal loss of activity, reinforcing the practical and environmental advantages of the methodology. Collectively, these findings establish the microwave-assisted HPW/PEG-400 platform as a potentially scalable, energy-efficient, and sustainable alternative for the rapid construction of bioactive 1,4-dihydropyridine frameworks, providing valuable guidance for the rational design of regioselective multicomponent heterocycle syntheses.

Supplementary Materials: The following supporting information can be downloaded at https://www.mdpi.com/article/10.3390/catal16010096/s1: detailed HRESI-MS (ESI-QTOF), ^{1}H NMR and ^{13}C NMR spectral data for compounds Figures S1–S16 and Table S1 is reported in reference [35,38,41,47–49]. CCDC-2517790 and CCDC-2517791 contain the supplementary crystallographic data for this paper. These data can be obtained free of charge from the Cambridge Crystallographic Data Centre via http://www.ccdc.cam.ac.uk/structures (accessed on 14 January 2026).

Author Contributions: Conceptualization, W.A.S. and S.C.S.T.; methodology, W.A.S., S.C.S.T., C.C.G. and I.V.M.; investigation, W.A.S., C.C.G. and I.V.M.; writing—review and editing, W.A.S., S.C.S.T., I.V.M. and C.C.G. All authors have read and agreed to the published version of the manuscript.

Funding: This work received financial support from the National Council of Technological and Scientific Development (CNPq), University of Brasilia (UnB).

Data Availability Statement: Data are contained within the article and Supplementary Materials.

Acknowledgments: The authors thank N.T.S., K.T.S., and IQ-UnB.

Conflicts of Interest: The authors declare no conflicts of interest.

Abbreviations

The following abbreviations are used in this manuscript:

DHP's	Dihydropyridines
HPW	Phosphotungstic acid
PEG	Polyethylene glycol
p-TsOH	*p*-toluenesulfonic acid
NADH	Nicotinamide adenine dinucleotide
NADPH	Nicotinamide adenine dinucleotide phosphate
IUPAC	International Union of Pure and Applied Chemistry
CCBs	Calcium-channel blockers
MCR	Multicomponent reaction
([Msim]Cl)	3-methyl-1-sulfonic acid imidazolium chloride
MW	Microwave
^{1}CNMR	proton nuclear magnetic resonance
^{13}CNMR	Carbon-13 nuclear magnetic resonance
MAOS	microwave-assisted organic synthesis
HPLC	High-performance liquid chromatography
ORTEP	Oak Ridge Thermal Ellipsoid Plot
TLC	Thin-layer chromatography
HRMS (ESI-QTOF)	high-resolution mass spectrometry performed using electrospray ionization–quadrupole time-of-flight

References

1. Khan, E. Pyridine derivatives as biologically active precursors: Organics and selected coordination complexes. *ChemistrySelect* **2021**, *6*, 3041–3064. [CrossRef]
2. Sahu, D.; Sreekanth, P.S.R.; Behera, P.K.; Pradhan, M.K.; Patnaik, A.; Salunkhe, S.; Cep, R. Advances in synthesis, medicinal properties and biomedical applications of pyridine derivatives: A comprehensive review. *Eur. J. Med. Chem. Rep.* **2024**, *12*, 100210. [CrossRef]
3. Choudhary, S.; Kumari, A.; Kumar, R.; Kumar, S.; Singh, R.K. Progress in nitrogen and oxygen-based heterocyclic compounds for their anticancer activity: An update (2017–2020). In *Key Heterocyclic Cores for Smart Anticancer Drug-Design Part I*; Bentham Science Publishers: Sharjah, United Arab Emirates, 2022; pp. 232–259. [CrossRef]
4. Kerru, N.; Gummidi, L.; Maddila, S.; Gangu, K.K.; Jonnalagadda, S.B. A review on recent advances in nitrogen-containing molecules and their biological applications. *Molecules* **2020**, *25*, 1909. [CrossRef]
5. Mathur, R.; Negi, K.S.; Shrivastava, R.; Nair, R. Recent developments in the nanomaterial-catalyzed green synthesis of structurally diverse 1,4-dihydropyridines. *RSC Adv.* **2021**, *11*, 1376–1393. [CrossRef]
6. Samrat, A.K.; Pratibha, B.A. 1,4-Dihydropyridines: A class of pharmacologically important molecules. *Mini-Rev. Med. Chem.* **2014**, *14*, 282–290. [CrossRef]
7. Pinder, A.R. An alkaloid of *Dioscorea hispida*, Dennst. *Nature* **1951**, *168*, 1090. [CrossRef]
8. Lavilla, R. Recent developments in the chemistry of dihydropyridines. *J. Chem. Soc. Perkin Trans. 1* **2002**, *9*, 1141–1156. [CrossRef]
9. Nakano, H.; Osone, K.; Takeshita, M.; Kwon, E.; Seki, C.; Matsuyama, H.; Takano, N.; Kohari, Y. A novel chiral oxazolidine organocatalyst for the synthesis of an oseltamivir intermediate using a highly enantioselective Diels–Alder reaction of 1,2-dihydropyridine. *Chem. Commun.* **2010**, *46*, 4827–4829. [CrossRef] [PubMed]
10. Triggle, D.J. Calcium channel antagonists: Clinical uses—Past, present and future. *Biochem. Pharmacol.* **2007**, *74*, 1–9. [CrossRef]
11. Malhi, D.S.; Kaur, N.; Kaur, M.; Han, H.; Bhowmik, P.K.; Husain, F.M.; Sohal, H.S.; Verma, M. Synthesis and antimicrobial activity of chalcone-derived 1,4-dihydropyridine derivatives using magnetic Fe_2O_3@SiO_2 as highly efficient nanocatalyst. *Catalysts* **2025**, *15*, 281. [CrossRef]
12. Brūvere, I.; Bisenieks, E.; Poikans, J.; Uldrikis, J.; Plotniece, A.; Pajuste, K.; Rucins, M.; Vīgante, B.; Kalme, Z.; Gosteva, M.; et al. Dihydropyridine derivatives as cell growth modulators in vitro. *Oxid. Med. Cell. Longev.* **2017**, *2017*, 4069839. [CrossRef]
13. Nakayama, H.; Kanaoka, Y. Chemical identification of binding sites for calcium channel antagonists. *Heterocycles* **1996**, *42*, 901–909. [CrossRef]

14. Sambongi, Y.; Nitta, H.; Ichihashi, K.; Futai, M.; Ueda, I. A novel water-soluble Hantzsch 1,4-dihydropyridine compound that functions in biological processes through NADH regeneration. *J. Org. Chem.* **2002**, *67*, 3499–3501. [CrossRef]
15. Pollak, N.; Dölle, C.; Ziegler, M. The power to reduce: Pyridine nucleotides—Small molecules with a multitude of functions. *Biochem. J.* **2007**, *402*, 205–218. [CrossRef] [PubMed]
16. Welsch, M.E.; Snyder, S.A.; Stockwell, B.R. Privileged scaffolds for library design and drug discovery. *Curr. Opin. Chem. Biol.* **2010**, *14*, 347–361. [CrossRef] [PubMed]
17. Pathak, S.; Jain, S.; Pratap, A. A review on synthesis and biological potential of dihydropyridines. *Lett. Drug Des. Discov.* **2024**, *21*, 15–33. [CrossRef]
18. Yedinak, K.C.; Lopez, L.M. Felodipine: A new dihydropyridine calcium-channel antagonist. *Ann. Pharmacother.* **1991**, *25*, 1109–1115. [CrossRef]
19. Allen, G.S.; Ahn, H.S.; Preziosi, T.J.; Battye, R.; Boone, S.C.; Chou, S.N.; Kelly, D.L.; Weir, B.K.; Crabbe, R.A.; Lavik, P.J.; et al. Cerebral Arterial Spasm—A Controlled Trial of Nimodipine in Patients with Subarachnoid Hemorrhage. *N. Engl. J. Med.* **1983**, *308*, 619–624. [CrossRef]
20. Manzar, A.; Sic, A.; Banh, C.; Knezevic, N.N. Therapeutic potential of calcium channel blockers in neuropsychiatric, endocrine and pain disorders. *Cells* **2025**, *14*, 1114. [CrossRef]
21. Abernethy, D.R.; Schwartz, J.B. Calcium-antagonist drugs. *N. Engl. J. Med.* **1999**, *341*, 1447–1457. [CrossRef] [PubMed]
22. Shimizu, H.; Nakagami, H.; Yasumasa, N.; Osako, K.M.; Kyutoku, M.; Koriyama, H.; Nakagami, F.; Shimamura, M.; Rakugi, H.; Morishita, R. Cilnidipine, but not amlodipine, ameliorates osteoporosis in ovariectomized hypertensive rats through inhibition of the N-type calcium channel. *Hypertens. Res.* **2012**, *35*, 77–81. [CrossRef] [PubMed]
23. Hantzsch, A. Condensation produkte aus Aldehydammoniak und ketonartigen Verbindungen. *Justus Liebigs Ann. Chem.* **1882**, *215*, 1–82. [CrossRef]
24. Li, P.; Wang, S.; Tian, N.; Yan, H.; Wang, J.; Song, X. Studies on chemoselective synthesis of 1,4- and 1,2-dihydropyridine derivatives by a Hantzsch-like reaction: A combined experimental and DFT study. *Org. Biomol. Chem.* **2021**, *19*, 1059–1070. [CrossRef]
25. Shen, L.; Cao, S.; Wu, J.; Zhang, J.; Li, H.; Liu, N.; Qian, X. A revisit to the Hantzsch reaction: Unexpected products beyond 1,4-dihydropyridines. *Green Chem.* **2009**, *11*, 1414–1420. [CrossRef]
26. Khan, S.; Siddiqui, Z.N. An efficient, green and solvent-free protocol for one-pot synthesis of 1,4-dihydropyridine derivatives using a new recyclable heterogeneous catalyst. *J. Mol. Struct.* **2023**, *1288*, 135758. [CrossRef]
27. Goswami, A.; Kaur, N.; Kaur, M.; Singh, K.; Sohal, H.S.; Han, H.; Bhowmik, P.K. Facile one-pot synthesis and anti-microbial activity of novel 1,4-dihydropyridine derivatives in aqueous micellar solution under microwave irradiation. *Molecules* **2024**, *29*, 1115. [CrossRef] [PubMed]
28. Safari, J.; Zarnegar, Z.; Mansouri-Kafroudi, Z. USY-zeolite catalyzed synthesis of 1,4-dihydropyridines under microwave irradiation: Structure and recycling of the catalyst. *J. Mol. Struct.* **2021**, *1227*, 129430. [CrossRef]
29. Soni, A.; Sharma, M.; Singh, R.K. A Decade of Catalytic Progress in 1,4-Dihydropyridines (1,4-DHPs) Synthesis (2016–2024). *Curr. Org. Synth.* **2025**, *22*, 703–720. [CrossRef]
30. Banerjee, S.; Horn, A.; Khatri, H.; Sereda, G. The solvent-free synthesis of 1,4-dihydropyridines under ultrasound irradiation without catalyst. *Ultrason. Sonochem.* **2008**, *15*, 677–680. [CrossRef]
31. Pathak, S.; Jain, S.; Pratap, A. 1,4-Dihydropyridine: Synthetic advances, medicinal and insecticidal properties. *RSC Adv.* **2022**, *12*, 29253–29290. [CrossRef]
32. Alvim, H.G.O.; Bataglion, G.A.; Ramos, L.M.; de Oliveira, A.L.; de Oliveira, H.C.B.; Eberlin, M.N.; de Macedo, J.L.; da Silva, W.A.; Neto, B.A.D. Task-specific ionic liquid incorporating anionic heteropolyacid-catalyzed Hantzsch and Mannich multicomponent reactions: Ionic liquid effect probed by ESI-MS(/MS). *Tetrahedron* **2014**, *70*, 3306–3313. [CrossRef]
33. Blázquez-Barbadillo, C.; González, J.F.; Porcheddu, A.; Virieux, D.; Menéndez, J.C.; Colacino, E. Benign synthesis of therapeutic agents: Domino synthesis of unsymmetrical 1,4-diaryl-1,4-dihydropyridines in the ball mill. *Green Chem. Lett. Rev.* **2022**, *15*, 881–892. [CrossRef]
34. Liu, F.-J.; Sun, T.-T.; Yang, Y.-G.; Huang, C.; Chen, X.-B. Divergent synthesis of dual 1,4-dihydropyridines with different substituted patterns from enaminones and aldehydes through domino reactions. *RSC Adv.* **2018**, *8*, 12635–12643. [CrossRef]
35. Bosica, G.; Demanuele, K.; Padrón, J.M.; Puerta, A. One-pot multicomponent green Hantzsch synthesis of 1,2-dihydropyridine derivatives with antiproliferative activity. *Beilstein J. Org. Chem.* **2020**, *16*, 2869–2876. [CrossRef] [PubMed]
36. Tiwari, S.K.; Shivhare, K.N.; Patel, M.K.; Yadav, V.; Nazeef, M.; Siddiqui, I.R. A metal-free Hantzsch synthesis for the privileged scaffold 1,4-dihydropyridines: A glycerol-promoted sustainable protocol. *Polycycl. Aromat. Compd.* **2020**, *40*, 1035–1047. [CrossRef]
37. Jassem, A.M.; Almashal, F.A.K.; Mohammed, M.Q.; Jabir, H.A.S. A catalytic and green method for one-pot synthesis of new Hantzsch 1,4-dihydropyridines. *SN Appl. Sci.* **2020**, *2*, 359. [CrossRef]
38. Erşatır, M.; Türk, M.; Giray, E.S. An efficient and green synthesis of 1,4-dihydropyridine derivatives through multicomponent reaction in subcritical ethanol. *J. Supercrit. Fluids* **2021**, *176*, 105303. [CrossRef]

39. Pachipulusu, S.; Merugu, K.S.; Bhonsle, R.R.; Kurnool, A.A. A facile microwave-mediated method of 1,4-dihydropyridine carboxylates synthesis by multicomponent reaction. *J. Heterocycl. Chem.* **2024**, *61*, 1009–1014. [CrossRef]
40. Silva, W.A.; Takada, S.C.S.; Nogueira, F.M.; Almeida, L.A.R. Microwave-assisted catalytic transfer hydrogenation of chalcones: A green, fast, and efficient one-step reduction using ammonium formate and Pd/C. *Organics* **2025**, *6*, 40. [CrossRef]
41. Morales, J.E.T.; Villavicencio, C.B.; Cervantes, X.L.G.; Canchingre, M.E.; Pedroso, M.T.C. Oxidative aromatization of some 1,4-dihydropyridine derivatives using pyritic ash in eco-sustainable conditions. *Chem. Proc.* **2023**, *14*, 61. [CrossRef]
42. Dolomanov, O.V.; Bourhis, L.J.; Gildea, R.J.; Howard, J.A.K.; Puschmann, H. OLEX2: A complete structure solution, refinement and analysis program. *J. Appl. Crystallogr.* **2009**, *42*, 339–341. [CrossRef]
43. Sheldrick, G.M. A short history of SHELX. *Acta Crystallogr. Sect. A* **2008**, *64*, 112–122. [CrossRef] [PubMed]
44. Sheldrick, G.M. Crystal structure refinement with SHELXL. *Acta Crystallogr. Sect. C* **2015**, *71*, 3–8. [CrossRef]
45. Sheldrick, G.M. *SADABS: Program for Empirical Absorption Correction of Area Detector Data*; University of Göttingen: Göttingen, Germany, 1997.
46. Macrae, C.F.; Sovago, I.; Cottrell, S.J.; Galek, P.T.A.; McCabe, P.; Pidcock, E.; Platings, M.; Shields, G.P.; Stevens, J.S.; Towler, M.; et al. Mercury 4.0: From visualization to analysis, design and prediction. *J. Appl. Crystallogr.* **2020**, *53*, 226–235. [CrossRef]
47. Prasanthi, G.; Prasad, K.V.S.R.G.; Bharathi, K. Design, Synthesis and Evaluation of Dialkyl 4-(benzo[d][1,3]dioxol-6-yl)-1,4-dihydro-2,6-dimethyl-1-substituted Pyridine-3,5-dicarboxylates as Potential Anticonvulsants and Their Molecular Properties Prediction. *Eur. J. Med. Chem.* **2013**, *66*, 516–525. [CrossRef] [PubMed]
48. Salazar, R.; Navarrete-Encina, P.A.; Camargo, C.; Squella, J.A.; Núñez-Vergara, L.J. Electrochemical Oxidation of C4-Vanillin- and C4-Isovanillin-1,4-dihydropyridines in Aprotic Medium: Reactivity towards Free Radicals. *J. Electroanal. Chem.* **2008**, *622*, 29–36. [CrossRef]
49. Loev, B.; Snader, K.M. The Hantzsch Reaction. I. Oxidative Dealkylation of Certain Dihydropyridines. *J. Org. Chem.* **1965**, *30*, 1914–1916. [CrossRef]